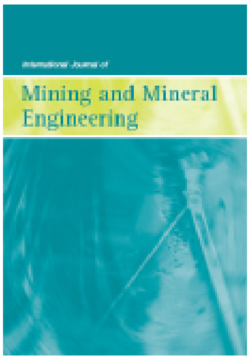

International Journal of Mining and Mineral Engineering

ISSN online: 1754-8918 - ISSN print: 1754-890X
https://www.inderscience.com/ijmme

Mechanism study on the sandstone roof caving characteristics for improving the preconditioning measures to mitigate the windblast risk in coal mines

Jinhe Jia, Zhichao Wang, Zhen Zhang

DOI: 10.1504/IJMME.2024.10063644

Article History:

Received:	18 August 2023
Last revised:	07 February 2024
Accepted:	28 February 2024
Published online:	29 May 2024

Mechanism study on the sandstone roof caving characteristics for improving the preconditioning measures to mitigate the windblast risk in coal mines

Jinhe Jia* and Zhichao Wang

CCTEG Coal Mining Research Institute,
Beijing, 100013, China
Email: jjhjll@sina.com
Email: wangzhichao@tdkcsj.com
*Corresponding author

Zhen Zhang

Coal Mining and Designing Department,
Tiandi Science and Technology Co., Ltd.,
Beijing, 100013, China
Email: zhangzhen@tdkcsj.com

Abstract: The geological feature of sandstone strata directly overlying coal seams is common in the Shendong shallow buried coal field, and causes delayed roof caving and the risk of windblasts in the initial longwall mining stage. To mitigate windblasts, preconditioning measures, such as hydraulic fracturing operations and temporary blasting operations, are employed to improve the roof caving performance. Site observations show that the thicker the overburden, the more difficult the roof caving becomes, and the conditioning measures do not produce very good roof caving performance as expected when the overburden thickness approaches 200 m. Numerical simulations are employed to investigate the roof-caving mechanism associated with the geological conditions of the Shendong coal field. The numerical results show that structurally controlled instability is the main mechanism of the roof caving; the gravitationally-loaded horizontal stress can lead to worse roof caving performance in the case of greater overburden thickness.

Keywords: first roof caving; sandstone-dominated strata; hydraulic fracturing; horizontal stress; numerical simulation; windblast.

Reference to this paper should be made as follows: Jia, J., Wang, Z. and Zhang, Z. (2024) 'Mechanism study on the sandstone roof caving characteristics for improving the preconditioning measures to mitigate the windblast risk in coal mines', *Int. J. Mining and Mineral Engineering*, Vol. 15, No. 1, pp.49–70.

Biographical notes: Jinhe Jia received his PhD degree in Engineering Mechanics from University of Science and Technology Beijing, China in 2000. He is a Senior Engineer in the CCTEG Coal Mining Research Institute. His research interests include coal mining ground control techniques and numerical simulations.

Zhichao Wang received his Master degree in Mining Engineering from the China Coal Research Institute, Beijing in 2015. He is an engineer and a project manager in the CCTEG Coal Mining Research Institute. Currently, he is in charge of hydraulic fracturing projects and roadway support projects.

Zhen Zhang received his PhD degree in Mining Engineering from the China Coal Research Institute, Beijing in 2011. He is the director of the Roadway Support Branch, Coal Mining and Designing Department, Tiandi Science and Technology Co., Ltd. His research interests include techniques and theories of roadway support.

1 Introduction

The longwall coal mining systems with roof full caving are widely employed worldwide. The timely roof caving is significant for the normal operation of the longwall mining system. In the case of coal seams overlain by massive strata, the roof caving line can lie far behind the progressive mining face. If the main roof is part of massive strata, delayed roof caving means the rising periodic weighting distance, which can lead to overloaded shield supports at the mining face, overloaded pillars between tail roadways (tailgates) and strong seismic events (Campoli et al., 1987; Chlebowski and Burtan, 2021; Haramy and McDonnell, 1988; Van Dyke et al., 2017; Zhou et al., 2021). If the immediate roof is part of the massive strata, the roof caving can be seriously delayed, and accompanying windblasts may occur at the mining face (Jeffrey and Mills, 2000; Wei, 2020; Yu, 2022). The delayed roof caving on a large scale poses a serious threat to the safety of personnel and equipment at the mining face, and preconditioning measures such as blasting and hydraulic fracturing are available to shorten the overextended weighting distance or bring the roof down directly (Jiang et al., 2014; Jendryś et al., 2021; Fan et al., 2012).

The prediction of roof-caving behaviours has been an important subject in the application of longwall mining system. Many researchers have addressed the longwall roof caving characteristics with respect to the hard and thick strata through empirical models (Wang et al., 2020), physical models (Wang et al., 2021), numerical simulations (Gale and Nemick, 1998; Singh and Singh, 2010; Li et al., 2021), and onsite measurement techniques (Kelly et al., 1998). Periodic roof caving activities or weighting cycles can be identified during the longwall mining. Some studies have been carried out to investigate the relationship between periodic roof caving activities and support pressures, and it has been found that roof caving activity is partly associated with the real-time leg pressure data of shield supports (Truemen et al., 2008; Langosch et al., 2003; Wang et al., 2019). A general point of view is periodic roof caving activities are caused by the evolution of sub-vertical fractures in the roof just behind the longwall face, which is regarded as the tensile failure of the roof strata. However, numerical simulation results and micro-seismic monitoring data have shown that shear failures in the roof develop regularly ahead of the longwall face, and the positions of shear failures can enter into the roof as deep as tens of metres (Kelly et al., 1998; Heasley et al., 2001). This suggests the periodic roof caving may be a mixed result of two failure mechanisms.

This research deals with the problem of the delayed roof caving in the Shendong coal field. The Shendong coal field lies in the west-northern part of China, where thick sandstone-dominated strata directly overlying shallow buried coal seams are very common. As a result, the thick sandstone roof does not cave easily in the initial stage of longwall mining, and this can lead to a huge area of roof suspension over the mined-out area. Windblasts will occur and bring impaction at the longwall face if the huge area of the roof collapses suddenly. To deal with this risk, hydraulic fracturing or blasting operations are carried out to cause the roof caving as early as possible so that caving debris can completely fill the gap between the floor and the roof.

According to tens of existing cases in the Shendong coal field, if the overburden thickness is about 100m, the single hydraulic fracturing operations can successfully avoid the occurrence of windblasts; however, if the overburden thickness approaches 200m or more, the combination of hydraulic fracturing and blasting operations still cannot prevent small scale windblasts from occurring. That means the roof caving becomes more difficult with the increase of the overburden thickness. The phenomena remain unexplained, which hinders the improvement of existing preconditioning measures to fight against windblasts. Site identification, case analysis, and numerical simulation are employed in this research to understand the mechanism behind the phenomena.

2 Experiences of the first roof full caving in the Shendong coal field

Thirteen underground coal mines operate in the Shendong coal field. The total output of 13 mines amounts to more than 200Mt/a; eight mines have an output of more than 10Mt/a; tens of new coal panels are initiated per year. Controlling the risk of windblasts in these mines is a demanding job, however, it is discussed less in the current literature.

2.1 Geological and mechanical features

Coal seams being mined in the Shendong coal field have a buried depth ranging from 80m to 300m. Core data show that coal seams being mined have an average thickness of 5~6m; sandstone layers account for more than 50% of total roof strata in thickness, and siltstone layers about 30%; in most cases, the single sandstone layer varying in thickness from 5m to 30m overlies on a coal seam immediately.

Many studies have been carried out to investigate mechanical properties of rocks in the Shendong coal field. A study was conducted to investigate the variation of rock properties among eight sedimentary periods, based on laboratory tests on core samples collected from the Bulianta coal mine, the Daliuta coal mine, and the Buertai coal mine, which all belong to the Shendong coal field (Li et al., 2016). Another study was carried out to investigate the mechanical properties of Jurassic sandstone obtained from the Buertai coal mine, and shows that the uniaxial compressive strengths of sandstone increase with the decrease of grain sizes (Chen et al., 2018). The relation among rock properties, sedimentary periods, and overburden thicknesses has been investigated through laboratory tests on rock samples collected from three panels of the Shendong coal field (Du and Peng, 2019). The influence of natural weak planes on the mechanical properties of sandstone has been studied based on laboratory tests of rock samples obtained from the Shendong coal field (Li et al., 2020). According to the results of these studies, the average uniaxial compressive strength of sandstone ranges from 20MPa to 70MPa, mainly dependent on the sedimentary periods, and the average uniaxial compressive strength of siltstone ranges from 35MPa to 70MPa.

The general geological and mechanical features of the Shendong coal field are favourable for longwall mining because roof strata are stable but not too rigid to collapse. But it is not the case in the initial stage of longwall mining when relatively stable roof strata are not easy to cave and cause the risk of windblasts.

2.2 Preconditioning measures and performance

In the Shendong coal field, windblasts caused by the massive roof caving activities ever caused casualties in the initial longwall mining stage (Li, 2005). Since then, blasting operations have been employed to control windblast accidents in the Shendong coal field (Li, 2005; Qin and Liu, 2006). Using blasting operations as the main preconditioning measures lasted about a decade in the Shendong coal field. In recent years, hydraulic fracturing operations have been widely employed to deal with the hard roof problem in China’s coal mines; on the other hand, the blasting seismicity has become a public concern. These factors lead to hydraulic fracturing operations largely replacing the blasting operations to control the windblast accidents in the Shendong coal field, leaving blasting operations as an auxiliary role.

Though blasting operations as the main preconditioning measures lasted a long period in the Shendong coal field, there were few detailed reports to review the roof caving performance. However, since hydraulic fracturing has been introduced, many cases have been gathered and documented. The existing cases of inducing roof caving through hydraulic fracturing operations in the Shendong coal field show an obvious tendency: the thicker the overburden, the more difficult the roof caving becomes. When the overburden thickness is less than 150 m, the single hydraulic fracturing operations can lead to a good caving performance as expected; however, when the overburden thickness exceeds 200 m, the roof caving becomes difficult even if more hydraulic fracturing boreholes are drilled, and moreover, small scale blasting operations are performed.

To clarify the difference of roof caving behaviours caused by overburden thickness in the Shendong coal field, three cases are selected out of existing cases: Panel 52604, with a face length of about 310m, in the Daliuta coal mine, and the two adjacent Panels 52307 and 52308, both with a face length of about 315m, in the Yujialiang coal mine. Panel 52604 has an overburden thickness of 115~130m, and Panels 52307 and 52308 have an overburden thickness of 200~220m. All the three panels belong to the same coal seam of the Shendong coal field, called Coal 5-2. The Coal 5-2’s thickness varies from 4.3m to 8.4 m, with an average of 6m. Figure 1 shows the Coal 5-2’s roof strata in the Yujialiang coal mine and the Daliuta coal mine, respectively, both having a thick sandstone direct roof with the uniaxial compressive strength ranging from 32 MPa to 48 MPa. Because the three panels belong to the same coal seam, the geological environment forming the roof sandstone strata is similar; therefore, the roof caving characteristics are more comparable among the three panels.

Figure 2(a) shows the top view of hydraulic fracturing boreholes for Panel 52604, and Figure 2(b) shows the side view of hydraulic fracturing boreholes drilled from the starting room. The diameter of hydraulic fracturing boreholes is 56 mm. Thirty three hydraulic fracturing boreholes were drilled from the starting room towards the mining direction, and ten were drilled from the ventilation roadway and the transport roadway, six normal to the mining direction and four diverted about 5º from the mining direction. These hydraulic fracturing boreholes can be classified into two types, labelled with numbers 1 and 2, and each type has the same length (L) and dip angle (β), as shown in

Table 1, in which n denotes the sum of each type. The boreholes of types 1 and 2 drilled from the starting room both have a spacing of 20m, and the boreholes of type 2 drilled from the ventilation roadway and the transport roadway have a spacing of 15m. The hydraulic fracturing operations were carried out between Nov. 2019 and Dec. 2019 before the mining operations of Panel 52604. The average hydraulic fracturing spacing along the boreholes is about 3m.

Table 1 Specifications of hydraulic fracturing boreholes

Borehole type no.	*Panel 52604*			*Panel 52307*			*Panel 52308*		
	L/m	*β(°)*	*n*	*L/m*	*β(°)*	*n*	*L/m*	*β(°)*	*n*
1	42	25	17	62	7	16	65	10	16
2	35	50	26	41	16	19	50	25	23
3	/	/	/	22	26	38	30	40	14
4	/	/	/	22	42	16	/	/	/
5	/	/	/	17	68	19	/	/	/

Figure 1 Roof strata in (a) the Yujialiang coal mine (b) the Daliuta coal mine

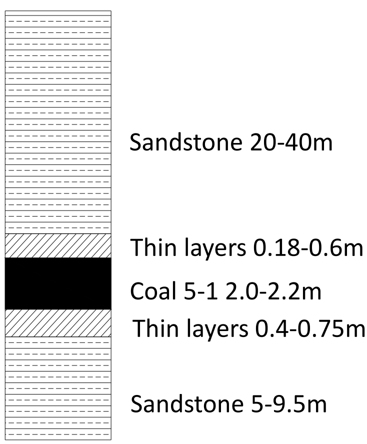

(a)

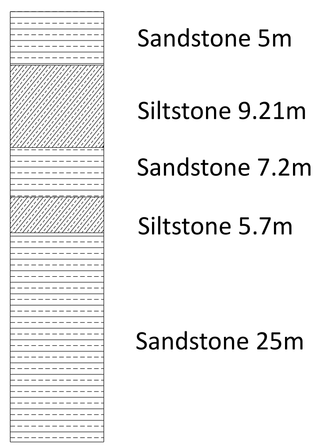

(b)

Figure 3(a) shows the top view of hydraulic fracturing boreholes for Panel 52307, and Figure 3(b) shows the side view of hydraulic fracturing boreholes drilled from the starting room. Ninety eight hydraulic fracturing boreholes were drilled from the starting room towards the mining direction; the boreholes of types 1 and 4 overlap and the boreholes of types 2 and 5 overlap in the top view. Ten hydraulic fracturing boreholes were drilled from the ventilation roadway, and the transport roadway, four overlapping boreholes in the top view normal to the mining direction, and six diverted about 5°from the mining direction. The boreholes of types 1, 2, 4, and 5 drilled from the starting room all have a spacing of 20m, but the boreholes of the type 3 have a spacing of 10m, and this leads to a spacing of 5m between boreholes in the top view. The boreholes of type 3, drilled from the ventilation roadway and the transport roadway, have a spacing of 20m. The hydraulic fracturing operations were carried out between Aug. 2021 and Sep. 2021 before the mining operations of Panel 52307. The average hydraulic fracturing spacing along the boreholes is about 3m, and the average hydraulic fracturing time at a point is about 30min.

Figure 4(a) shows the top view of hydraulic fracturing boreholes for Panel 52308, and Figure 4(b) shows the side view of hydraulic fracturing boreholes drilled from the starting room. Forty one hydraulic fracturing boreholes were drilled from the starting room towards the mining direction; 12 hydraulic fracturing boreholes were drilled from the ventilation roadway and the transport roadway. The boreholes of types 1 and 2 drilled from the starting room both have a spacing of 20m, but the boreholes of type 3 have a spacing of 10m. The boreholes of types 2 and 3, drilled from the ventilation roadway and the transport roadway, have a spacing of 20m. The hydraulic fracturing operations were carried out between September 2020 and October 2020 before the mining operations of Panel 52308. The average hydraulic fracturing spacing along the boreholes is about 3m, and the average hydraulic fracturing time at a point is about 30min.

Figure 2 The configuration of hydraulic fracturing boreholes in (a) and side-view of boreholes in (b) for Panel 52604 (not to scale) (see online version for colours)

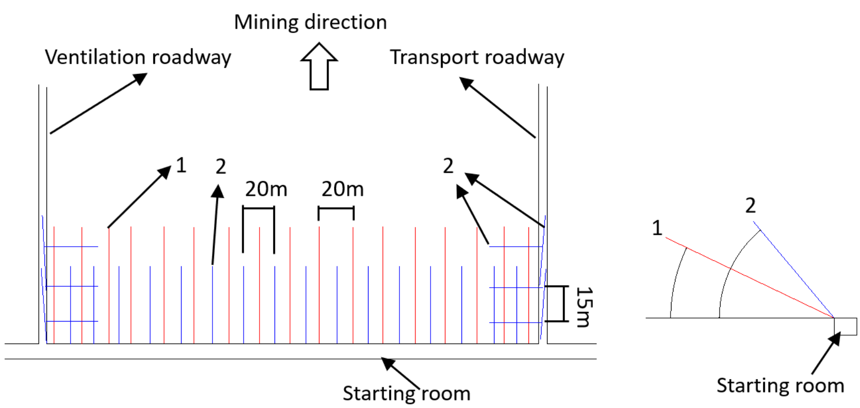

Figure 3 The configuration of hydraulic fracturing boreholes in (a) and side-view of boreholes in (b) for Panel 52307 (not to scale) (see online version for colours)

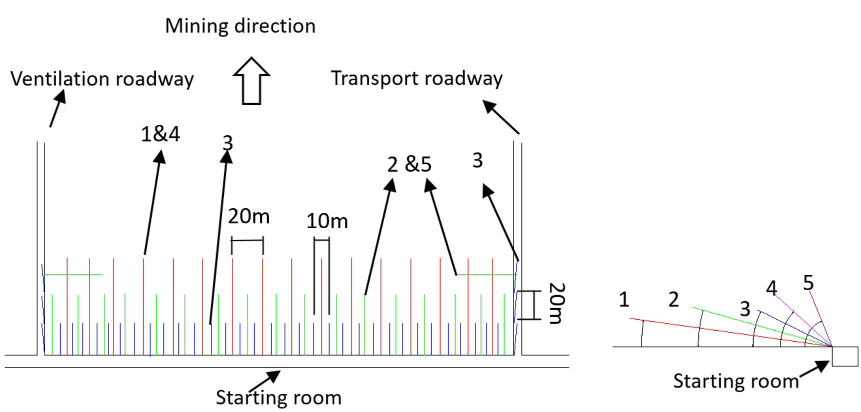

(a) (b)

Figure 4 The configuration of hydraulic fracturing boreholes in (a) and side-view of boreholes in (b) for Panel 52308 (not to scale)

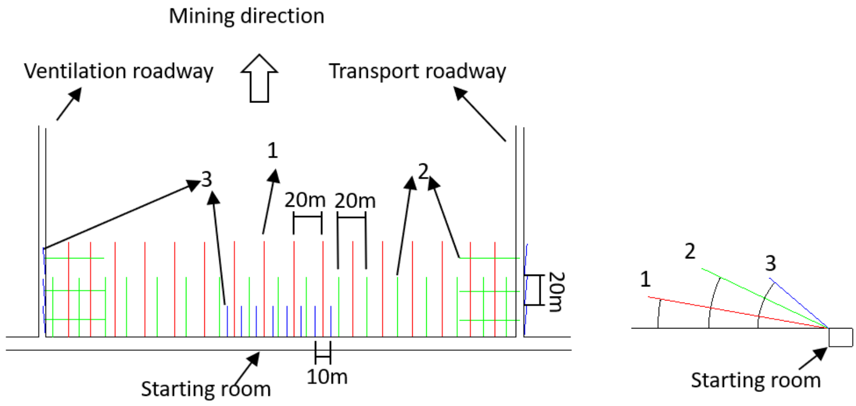

(a) (b)

The overburden thickness in Panels 52307 and 52308 surpasses 200m; the roof caving was expected to be more difficult. Therefore, the blasting operations on a small scale were employed. Figure 5 shows the pattern of the blasting boreholes: the blasting boreholes were drilled with a dip angle of 30º in the roof strata of the starting room before the longwall mining start, and the blasting boreholes largely lie on the same vertical plane and the spacing of blasting boreholes is 8 m. Table 2 shows the blasting parameters, where the decoupling ratio is charge diameter to blasting borehole diameter, and the charge ratio is charge length to blasting borehole length.

Figure 5 The pattern of the blasting boreholes for Panels 52307 and 52308 (see online version for colours)

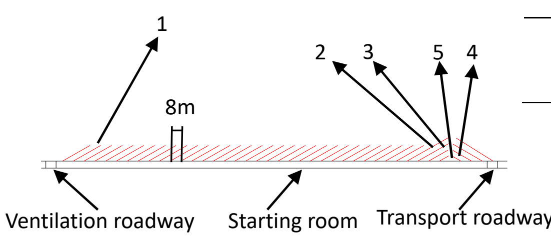

Parameter	Borehole type no.				
	1	2	3	4	5
L/m	20	32	24	16	8
β(º)	30	30	30	30	30
n	32	2	2	2	2

Table 2 Blasting parameters

Blasting hole diameter (mm)	*Charge diameter (mm)*	*Decoupling ratio (%)*	*Charge concentration (kg/m)*	*Charge ratio (%)*
85	35	41	3.0	0.7

Hydraulic fracturing operations in the above three panels were carried out before the longwall mining started. In Panel 52604, the hydraulic fracturing scope ranges about 38m in front of the starting room; in Panel 52307, the hydraulic fracturing scope ranges about 61 m; in Panel 52308, the hydraulic fracturing scope ranges about 64 m. Blasting operations in Panels 52307 and 52308 were carried out after the longwall face advanced about 6m.

Full-scale observations were performed to check the roof caving state behind the shield supports when the longwall face arrived at some given positions. The roof caving states are shown in Figures 6 through 8, where the solid thick lines represent the face positions when the observations were performed. According to Figure 6, obvious roof caving phenomena occurred in Panel 52604 when the longwall face advanced about 8m; the single hydraulic fracturing operations nearly resulted in a full roof caving when the longwall face advanced about 20m. However, no roof caving signs occurred in Panels 52307 and 52308 when the longwall face advanced about 6m, then blasting operations were carried out and induced roof caving activities. Obviously, delayed roof caving behaviours were always present in Panels 52307 and 52308 until the longwall face advanced about 60m. Besides, two small scale windblasts occurred in Panel 52307 and once in Panel 52308.

Figure 6 Schematic drawing of the roof caving in Panel 52604

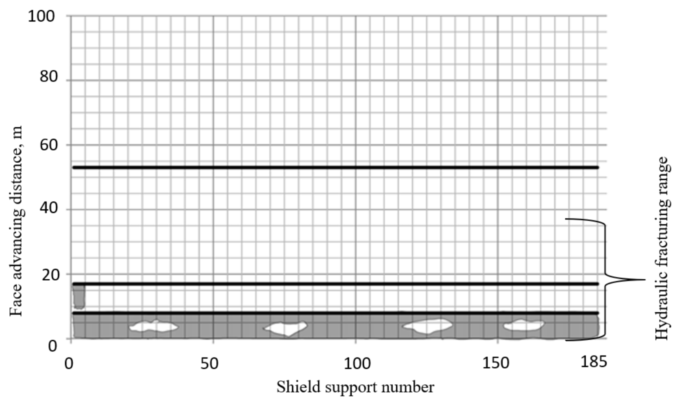

Figure 7 Schematic drawing of the roof caving in Panel 52307 (see online version for colours)

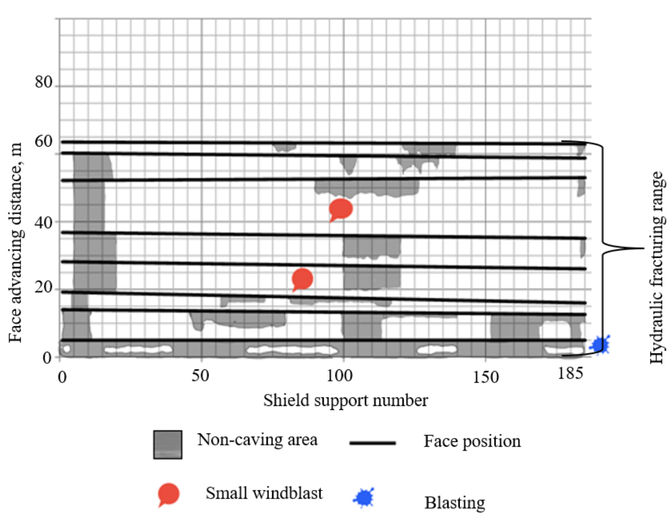

Figure 8 Schematic drawing of the roof caving in Panel 52308 (see online version for colours)

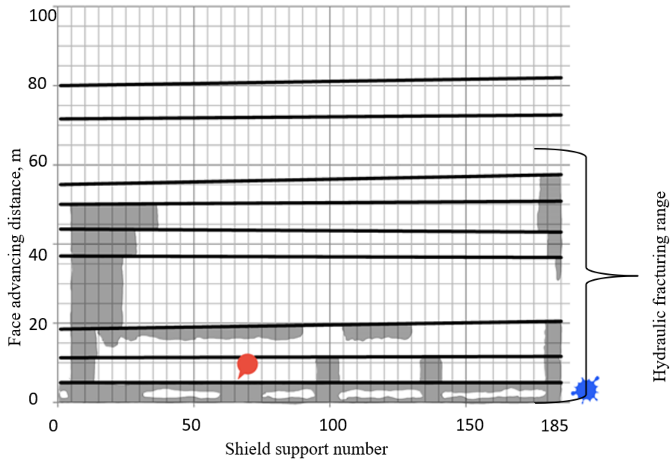

2.3 Comments

In the Shendong coal field, the roof caving characteristics displayed by the above three cases are typical for those cases with similar overburden thickness. Generally speaking, the existing preconditioning measures, including hydraulic fracturing and temporary blasting operations in the Shendong coal field can control the risk of windblasts to a low level. Nevertheless, the serious delayed roof caving cases occur occasionally. In these cases, normal mining activities have to be halted and temporary amending measures have to be employed. To further improve the preconditioning measures and the first roof caving performance, it is crucial to understand the main factors leading to delayed roof falls.

In the case of the Shendong coal field, the roof caving performance seems to have a close connection with overburden thickness: the bigger the overburden thickness, the poorer the roof caving performance is; this is contrary to our general knowledge about the roof stability. To understand the mechanism behind this phenomenon, the mechanical analysis of the roof caving is necessary. The numerical simulation method is best suitable for this job, because geological and mechanical properties can be conveniently adjusted to match the real roof caving performance. In the next section, a series of numerical tests will be conducted to offer an answer to this question.

Before the numerical tests, we need to identify some potential geological and geo-mechanical factors that affect the first roof caving. The initial stage of longwall mining can be regarded as the process of a roadway changing its span while the face is advancing; with the increase of span, the enlarged roadway gradually loses stability, and roof falls occur. Besides span, rock strength, in situ stress, and geologic discontinuity are major factors associated with roof falls of the roadway. As far as the first roof caving mechanisms in the Shendong coal field is concerned, rock failures are less likely to be the main mechanism because of the combination of shallow buried coal seams and stable roof strata composed of sandstone and siltstone layers; on the other hand, in view of the fact that the sandstone roof tends to collapse timely except the initial stage of longwall mining, it can be assumed that roof caving is mainly due to the structurally controlled instability. According to these analyses, discontinuity and overburden thickness are two obvious factors that should be considered in the numerical tests. In addition, horizontal stress is employed as the third factor affecting roof caving. In general, large horizontal stress is regarded as an adverse factor affecting roadway stability, but it is not the case in the current study, where horizontal stress is part of the normal force acting on the discontinuities, which is expected to deter the roof caving.

3 Numerical tests

3.1 Modelling method

The numerical simulations are conducted based on the current mining circumstances of the Shendong coal field: the overburden thickness of about 100 m and 200 m are typical; the rock strata are flat, and the gravitationally loaded stress regime is assumed, i.e. the ratio of horizontal stress to vertical stress (σ_h / σ_v) equal to μ / (1 − μ), where μ is Poisson's ratio; the core data and site roof caving observations show the spacing of discontinuity in the roof rock strata is largely varying between 300 mm ~ 700 mm. To understand how the overburden thickness affects the roof caving performance, two UDEC models with an overburden thickness of 100m and 200m, respectively, are created by employing the same model configuration, the same rock properties, and the gravitationally loaded stress regime. In addition, numerical simulations are carried out to investigate the varying roof caving characteristics due to the change in the discontinuity or the horizontal stress. Therefore, another two models, both with an overburden thickness of 100 m, are created; the two models are identical to the former model with an overburden thickness of 100m, except that one model employs the slightly altered discontinuity and the other model employs the non-gravitationally loaded stress regime. As a result, three models out of the four models employ the overburden thickness of 100m, and one model employs the overburden thickness of 200m; three models employ the same model configuration, though one model employs the slightly altered discontinuity; three models employ the gravitationally loaded stress regime. Employing such a model design plan will guarantee there is only one single factor making differences between two contrasting models.

To identify varying roof caving characteristics, the numerical models need to simulate the longwall face advancing step by step. A large mined-out area is formed with the increase of the longwall face advancing distance (FAD), and this will lead to roof instability and roof falls. After the roof falls, it is difficult for the numerical models to reach a high-level equilibrium state. In the UDEC models, the ratio of the maximum unbalanced force to the representative internal force, denoted by R, is used to determine the equilibrium state, and R = 1e-5 denotes an equilibrium state with relatively high precision (UDEC Universal Distinct Element Code, 2011b). In the current simulations, the standard of reaching the equilibrium state for each excavation step is as follows: if the models can reach the equilibrium state (R = 1e-5), the calculation stops; if the models cannot reach this equilibrium state, the calculation stops after cycles of 3e5.

3.2 Model description

The four models are created by the UDEC software and have the same dimensions, 300 m wide and 145 m high, as shown in Figure 9(a); the origin of coordinates (x, y) is 150 m away from the left boundary and 45m above the bottom boundary. For the three models with an overburden thickness of 100 m, the top boundary is free; for the model with an overburden thickness of 200 m, the top boundary is loaded with the vertical stress equivalent to 100 m overburden thickness. For all four models, the left and right boundaries are fixed in the horizontal direction, and the bottom boundary is fixed in the vertical direction. The black central area in Figure 9(a), 70 m wide and 24 m high, is divided by three sets of joints with dip angles of 0º, 60º, and 120º and the same spacing of 0.5 m, representing the regular roof rock structures, as shown in Figure 9(b). A slight change is performed in the joint continuity of Figure 9(b) by introducing a gap of 0.5m between joint segments of 2 m; Figure 9(c) shows the result of this change representing the irregular roof rock structures. Table 3 shows the main features of the four models, which have the names B100, B200, HB100, and HHS100, respectively. The B100 model denotes a typical mining condition with an overburden thickness of 100 m; the B200 model denotes a typical mining condition with an overburden thickness of 200 m; the Hb100 model employs the irregular roof structures as shown in Figure 9(c); the Hhs100 model employs the specified stress regime σ_h / σ_v = 1. Table 4 gives the properties of elastic models for rock blocks according to testing data, and Table 5 gives the joint properties for the rock structures, which are determined by trial and error to reflect the roof caving characteristics in the Shendong coal field.

Mesh size can affect the result of numerical simulations, and therefore, the numerical results should be checked before formal numerical simulations. For UDEC models, the mesh size of models is controlled by the average edge length of a zone (a triangle element). The edge length of 0.5 m can control the error of numerical results at a level of less than 1%, as compared with the analytic solutions of displacements (Jia, 2021). The numerical models in this research employ the edge length of 0.5 m in the centre area of interest, though the edge length of 2 m is employed outside the centre area. Hydraulic fracturing operations have been widely employed to induce hard roof caving in the coal mines in China (Lin et al., 2021; Sun et al., 2019); and site observations show that hydraulic fracturing operations can lead to hard roof caving occurring 5~10 m earlier than that in the non-hydraulic- fracturing area. Employing the geological and mechanical parameters in the Tables 3 through 5, the results of numerical simulations in this research are in agreement with the estimated roof caving state without employing preconditioning measures.

The pre-simulation procedure includes: assigning material constitutive models and material properties, applying boundary conditions, and stepping into an initial equilibrium state. Then the formal simulation is performed: the starting room is excavated, as shown in Figure 10, and subsequent excavations (longwall mining) produce a continuously enlarged mined-out area, which leads to the roof caving.

Figure 9 (a) Model configuration (b) regular roof structures (c) irregular roof structures

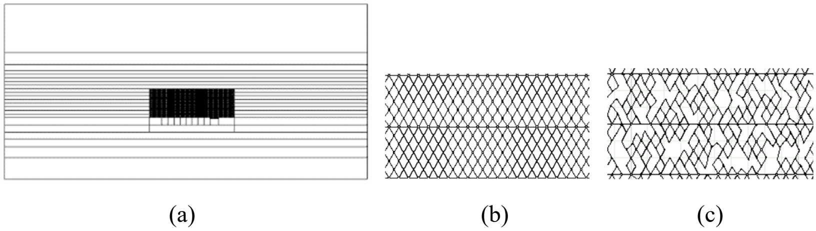

Table 3 Model features

Model name	*Overburden thickness (m)*	*Roof structure*	*Stress regime (σ_h / σ_v)*
B100	100	Regular	$\mu / (1 - \mu)$
B200	200	Regular	$\mu / (1 - \mu)$
Hb100	100	Irregular	$\mu / (1 - \mu)$
Hhs100	100	Regular	1

Table 4 Rock properties

Rock type	*Bulk modulus (Pa)*	*Shear modulus (Pa)*	*Density (kg/m^3)*
Sandstone	5e9	3e9	2,200
Siltstone	4.5e9	2.7e9	2,200
Coal	1.33e9	8e8	1,400
Claystone	2.0e9	1.2e9	2,200

Table 5 Joint properties

Property	*Value*
Normal stiffness (Pa/m)	1e11
Shear stiffness (Pa/m)	1e11
Friction angle (°)	30
Cohesion (Pa)	1e6
Tensile strength (Pa)	2e5

Figure 10 Longwall mining beginning with the starting room

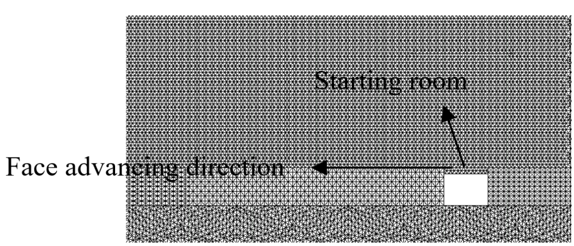

3.3 Results

Figures 11 through 14 show the roof caving state at specified FADs through displacement magnitude contours. All plots in Figures 11 through 14 use the same set of fill colours to represent displacements, as shown in Figure 11(i). In the case of B100, the roof caving begins on a large scale at FAD = 15 m, while in the case of B200, the roof caving begins on a small scale at FAD = 20 m. In the case of HB100, the roof caving begins on a large scale at FAD = 20 m, which shows that irregular roof structures, including many large rock blocks, delay the roof caving. In the case of HHS100, the roof caving begins at FAD = 40 m. If we overlook the fall of a small block of top coal above the roadway, this shows the higher horizontal stress can cause seriously delayed roof caving. The fact reminds us the difference between the two cases of B100 and B200 is very likely caused by the horizontal stress, which varies with the overburden thickness because all other parameters for the two cases are identical.

Then, a quantitative evaluation of the roof caving state has been performed, which will disclose more hidden information in the above plots. Using the UDEC built-in FISH programming language (UDEC Universal Distinct Element Code, 2011a), new functions and variables are defined to obtain the extra information from the models, such as the unstable roof area (URA). Herein, we define the unstable roof as a piece of roof with a more than 0.05 m displacement. Figure 15 shows the curves of URA versus FAD for four models, and the curves show the case of B100 has a larger URA in the early stage but is surpassed by the cases of B200 and HB100 in the later stage. Figure 16 shows the curves of the ratio of unstable roof area to mined-out area (URA/MOA) versus FAD for four models, and the curves show the case of B100 has a URA/MOA more than 1 at FAD = 15 m, while the case of B200 has a URA/MOA more than 1 at FAD = 25 m. Figure 17 shows the curves of the newly developed unstable roof area (NDURA) versus FAD for four models, and the curves show the case of B100 has a single peak of NDURA in the early stage, while the case of B200 has two peaks of NDURA in the later stage and the case of HB100 has a quickly and stably rising NDURA in the later stage. Figure 18 shows the curves of the unstable roof depth (URD) versus FAD for four models, and the curves show the case of B100 has a relatively stable UDR since the first large-scale roof caving in the early stage, while the cases of B200 and HB100 have a larger UDR in the later stage.

Figure 11 Roof caving for B100: (a) FAD = 5 m (b) FAD = 10 m (c) FAD = 15 m (d) FAD = 20 m (e) FAD = 25 m (f) FAD = 30 m (g) FAD = 30 m (h) FAD = 30 m (i) fill colours (see online version for colours)

(a)

(b)

Figure 11 Roof caving for B100: (a) FAD = 5 m (b) FAD = 10 m (c) FAD = 15 m (d) FAD = 20 m (e) FAD = 25 m (f) FAD = 30 m (g) FAD = 30 m (h) FAD = 30 m (i) fill colours (continued) (see online version for colours)

(c)

(d)

(e)

(f)

(g)

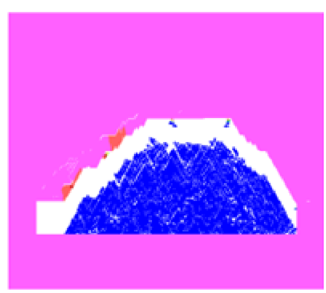

(h)

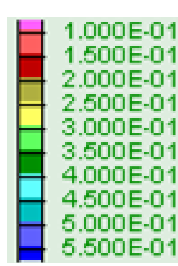

(i)

Figure 12 Roof caving for B200: (a) FAD = 5 m (b) FAD = 10 m (c) FAD = 15 m (d) FAD = 20 m (e) FAD = 25 m (f) FAD = 30 m (g) FAD = 35 m (h) FAD = 40 m (see online version for colours)

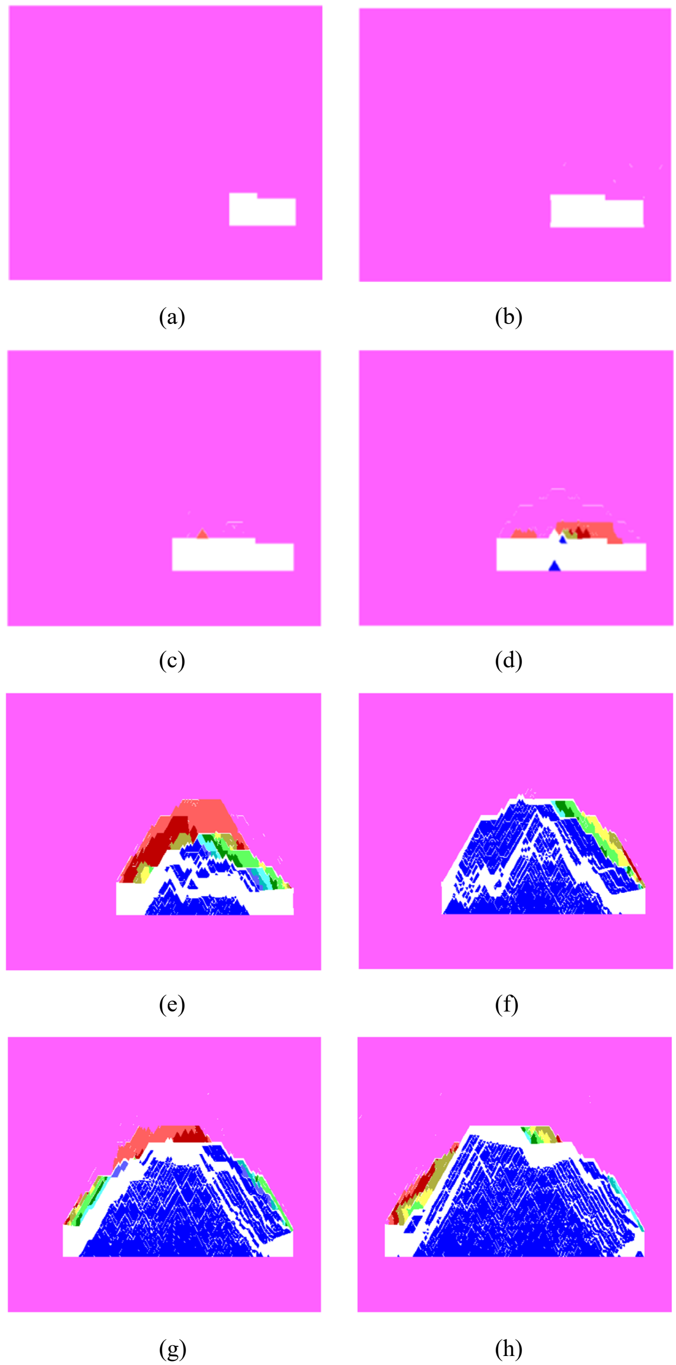

Figure 13 Roof caving for HB100: (a) FAD = 5 m (b) FAD = 10 m (c) FAD = 15 m (d) FAD = 20 m (e) FAD = 25 m (f) FAD = 30 m (g) FAD = 35 m (h) FAD = 40 m (see online version for colours)

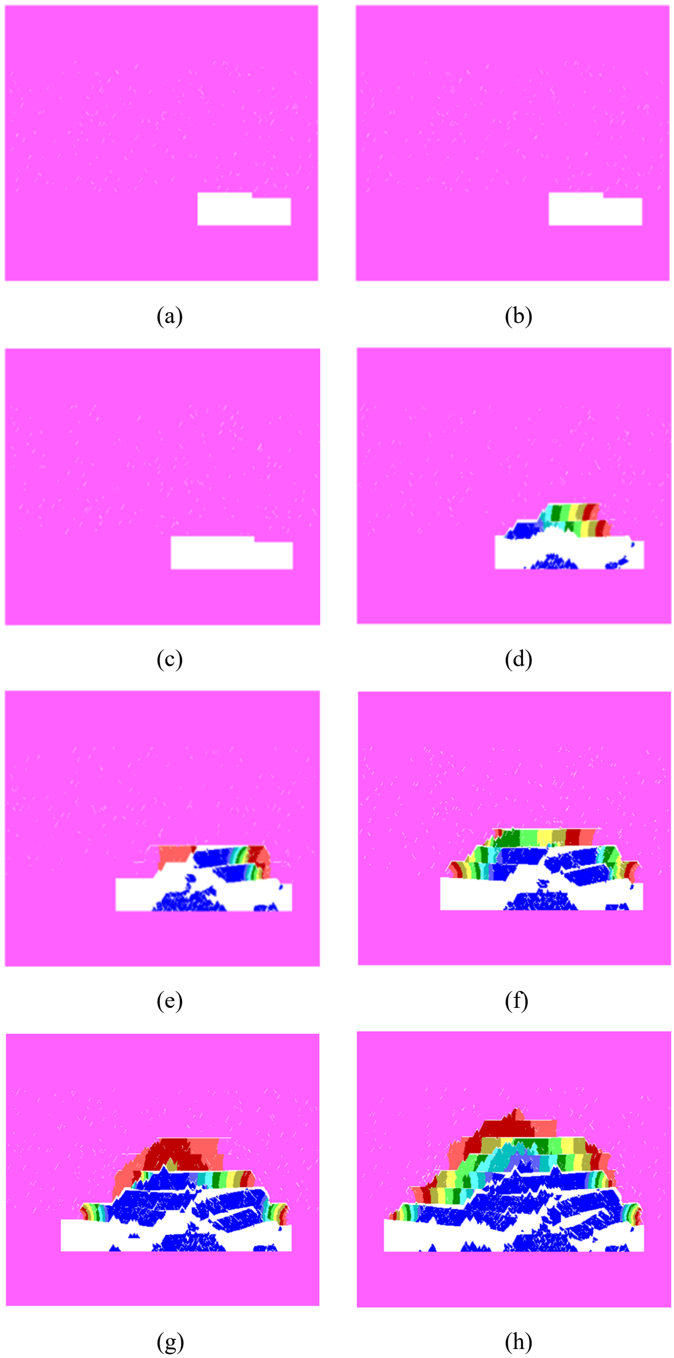

Figure 14 Roof caving for HHS100: (a) FAD = 5 m (b) FAD = 10 m (c) FAD = 15 m (d) FAD = 20 m (e) FAD = 25 m (f) FAD = 30 m (g) FAD = 35 m (h) FAD = 40 m (see online version for colours)

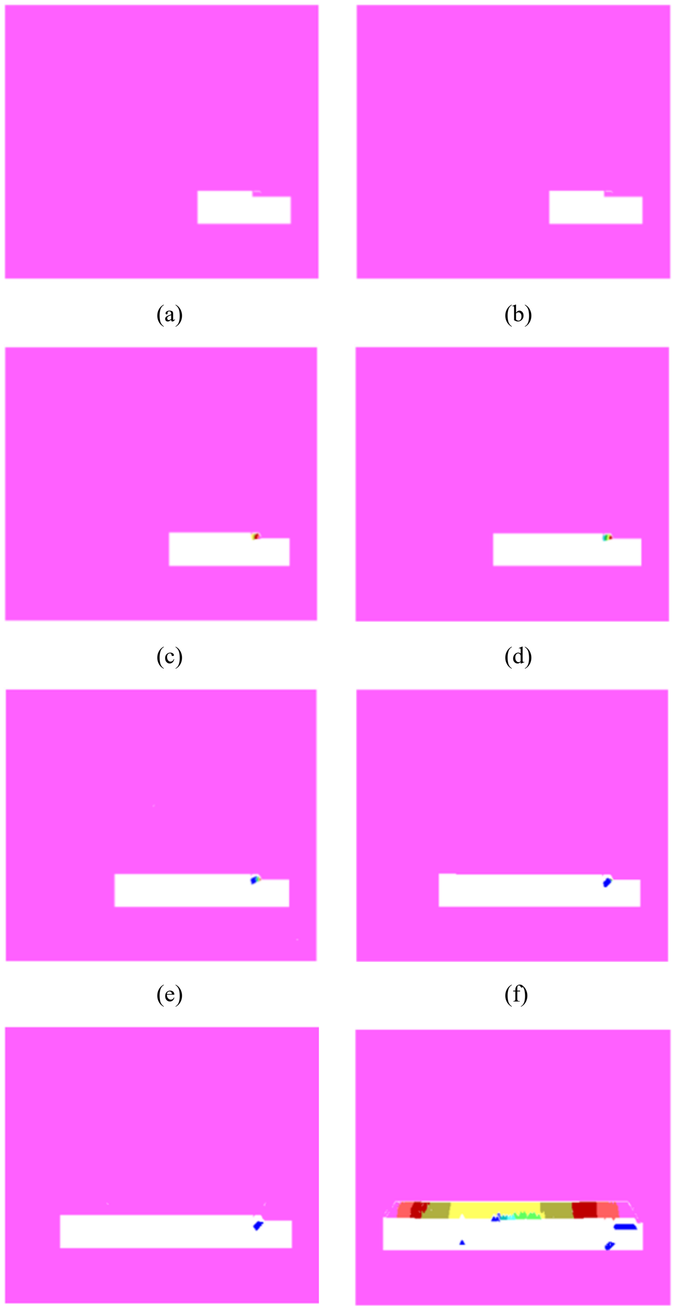

(a) (b) (c) (d) (e) (f) (g) (h)

Figure 15 Curves of URA versus FAD (see online version for colours)

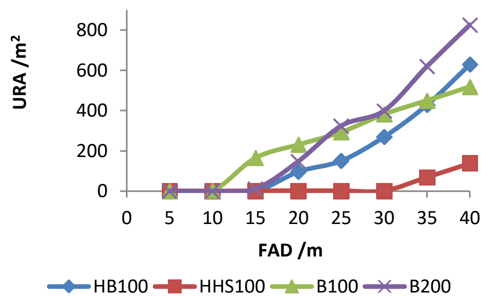

Figure 16 Curves of URA/MOA versus FAD (see online version for colours)

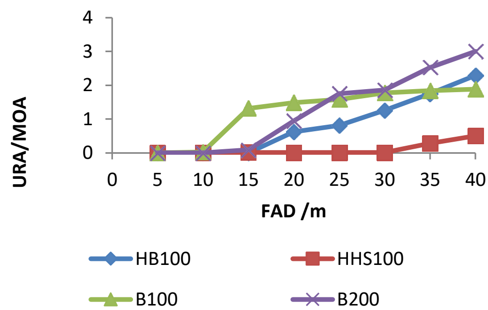

Figure 17 Curves of NDURA versus FAD (see online version for colours)

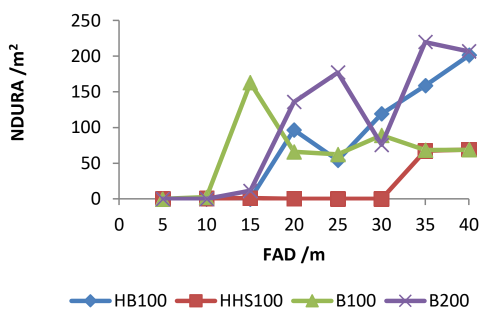

Figure 18 Curves of URD versus FAD (see online version for colours)

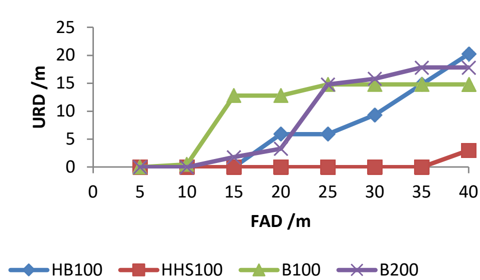

4 Discussion

For underground coal mining, thicker overburden generally means more unstable roof conditions, because high horizontal stress is the main factor to cause roof failure, especially when the direct roof is claystone, which degrades in strength quickly after exposure to air. Because of the sandstone direct roof and shallowly buried seams in the Shendong coal field, thicker overburden accompanies more difficult caving conditions. The above numerical results show that the increase in horizontal stress leads to roof caving becoming more difficult when the overburden thickness changes from 100 m to 200m. This can largely explain the roof caving characteristics in the Shendong coal field, seemingly dependent on the overburden thickness but on the horizontal stress.

At present, hydraulic fracturing techniques are widely employed to weaken the hard roof in China's coal mines. However, hydraulic fracturing operations theoretically only produce long-extended fractures with fixed direction in the roof strata, and the hydraulic fracturing spacing of 2~3 m is common, which is far more than the common joint spacing of coal measure rocks. Therefore, the function of hydraulic fracturing operations is the creation of large-scale fractures, but is not to induce roof to fall down instantly.

Blasting operations can produce lots of fractures in the roof strata in varied directions. However, in the Shendong coal field, blasting operations are discouraged by the management, and only small-scale blasting operations are allowed when they are thought necessary. As shown in Figure 6, the current blasting plan can only produce small circular fractured zones around the blasting holes, leaving most of the gap between the blasting boreholes intact.

In the cases of Panels 52307 and 52308, the combination of hydraulic fracturing and blasting operations were expected to create more fractures than that in the case of Panel 52604. However, the roof caving performance of the former is clearly worse than that of the latter. The possible reason is that the combination of hydraulic fracturing and blasting operations in the former does not greatly increase the density of fractures in the direct roof strata, as opposed to that in the latter; however, the increase of horizontal stress in the former lead to the difficulty of the roof caving rising greatly.

According to the mechanism of the roof caving in the Shendong coal field, an idealised strategy for improving the roof caving performance is: to create a narrow densely-fractured area in the direct roof, which is parallel to the starting room; once the longwall face advances past the densely-fractured area, the roof strata in this area cave quickly and the influence of horizontal stress disappears afterward. The difficulty in performing this strategy is finding feasible preconditioning measures which should be safe and economical. The results of this study are expected to be helpful in improving the preconditioning measures in the Shendong coal field.

5 Conclusions

In the Shendong shallow buried coal field, the delayed caving of the sandstone-dominated roof in the initial longwall mining stage can lead to windblasts. The hydraulic fracturing operations and temporary blasting operations are necessary in the initial longwall mining stage to mitigate this risk. In general, these practices effectively lower the risk of windblasts. But a baffling phenomenon remains unanswered because the site practices show a strange feature: the bigger the overburden thickness, the poorer the roof caving performance is, even if the more intensive hydraulic fracturing operations and temporary blasting operations are performed in the mines with a bigger overburden thickness. To improve the existing preconditioning measures, it is important to understand the mechanism behind this phenomenon.

To explain this phenomenon, the UDEC models are created to investigate the influence of overburden thickness, rock structure (joint distribution), and horizontal stress on the roof caving performance; the numerical simulations are performed with an assumption: the roof caving is the result of structurally controlled instability. The numerical results show that the horizontal stress that is proportional to the overburden thickness can explain the difference in the roof caving performance between varying overburden thicknesses; less joint continuity can deteriorate the roof caving performance, and this can partly explain the difference in the roof caving performance between two adjacent coal panels where roof structures are non-uniform; high horizontal stress can seriously deteriorate the roof caving performance.

References

Campoli, A.A., Kertis, C.A. and Goode, C.A. (1987) 'Coal mine bumps: five case studies in the eastern United States. United States department of the interior', *Information Circular*, Vol. 9149, p.34.

Chen, J., Lin, Z., Wang, Z., Huang, Y. and Li, Y. (2018) 'Characteristics of Jurassic sedimentary rocks and its influence on physico-mechanical property in Buertai Mine', *Coal Science and Technology*, Vol. 46, No. 2, pp.28–34.

Chlebowski, D. and Burtan, Z. (2021) 'Mining-induced seismicity during development works in coalbeds in the context of forecasts of geomechanical conditions', *Energies*, Vol. 14, No. 20, p.6675.

Du, F. and Peng, S.S. (2019) 'Change rule of physical and mechanical property of rock mass in Shendong mine', *Journal of Mining & Safety Engineering*, Vol. 36, No. 5, pp.1009–1015.

Fan, J., Dou, L., He, H., Du, T., Zhang, S., Gui, B. and Sun, X. (2012) 'Directional hydraulic fracturing to control hard-roof rockburst in coal mines', *Int. J. Min. Sci. Technol.*, Vol. 22, No. 2, pp.177–181.

Gale, W.J. and Nemick, J.A. (1998) 'Prediction of strata caving characteristics and its impact on longwall operation', *Coal98 Conference Wollongong*, 18–20 February, pp.156–166.

Haramy, K.H. and McDonnell, J.P. (1988) 'Causes and control of coal mine bumps', *USBM RI*, Vol. 9225, 35pp.

Heasley, K.A., Ellenberger, J.L. and Jeran, P.W. (2001) 'An analysis of rock failure around a deep longwall using micro-seismic', *Proceedings of the 20th Conference on Ground Control in Mining*, pp.280–286, West Virginia University, Morgantown, WV.

Jeffrey, R.G. and Mills, K.W. (2000) 'Hydraulic fracturing applied to inducing longwall coal mine goaf falls', *4th North American Rock Mechanics Symposium*, American Rock Mechanics Association.

Jendryś, M., Hadam, A. and Ćwiękała, M. (2021) 'Directional hydraulic fracturing (DHF) of the roof, as an element of rock burst prevention in the light of underground observations and numerical modelling', *Energies*, Vol. 14, No. 3, p.562.

Jia, J. (2021) 'Numerical analysis of ground support systems subjected to dynamic loading', *2021 IOP Conf Ser: Earth Environ Sci.*, Vol. 861, No. 3, p.032109.

Jiang, J., Dai, J., Wang, P. et al. (2014) 'Overlying hard and thick strata breaking movement and broken-roof control', *Rock and Soil Mechanics*, Vol. 35, No. S1, pp.264–270.

Kelly, M., Gale, W., Hatherly, P., Balusu, R. and Luo, X. (1998) 'Combining modern assessment methods to improve understanding of longwall geomechanics', in Aziz, N (Ed.): *Coal 1998: Coal Operators' Conference*, University of Wollongong & the Australasian Institute of Mining and Metallurgy, pp.523–535.

Langosch, U., Ruppel, U. and Wyink, U. (2003) 'Longwall roof control by calculation of the shield support requirements', in Aziz, N. (Ed.): *Coal 2003: Coal Operators' Conference, University of Wollongong & the Australasian Institute of Mining and Metallurgy*, pp.162–172.

Li, H. (2005) 'A preliminary investigation on the techniques of inducing the thick bedrock roof caving in the Shendong coal field', *Shaanxi Meitan*, Vol. 24, No. 2, pp.33–34.

Li, H., Li, H. and Xu, G. (2020) 'Study on mechanical characteristics of sandstone with natural weak plane in Shendong coal field', *Journal of Henan Polytechnic University (Natural Science)*, Vol. 39, No. 5, pp.10–17.

Li, H., Li, H., Song, G. and Wang, K. (2016) 'Physical and mechanical properties of the coal-bearing strata rock in Shendong coal field', *Journal of China Coal Society*, Vol. 41, No. 11, pp.2661–2671.

Li, Y., Ren, Y., Wang, N. et al. (2021) 'Structure form and evolution characteristics of collapsed roof in goaf', *Journal of China Coal Society*, Vol. 46, No. 12, pp.3771–3780.

Lin, J., Guo, K., Sun, Z. and Wang, T. (2021) 'Study on fracturing timing of hydraulic fracturing top-cutting and pressure relief in roadway with strong dynamic pressure', *Journal of China Coal Society*, Vol. 46, No. S1, pp.140–148.

Qin, Y. and Liu, J. (2006) 'The design and discussion of the artificial roof caving plan in the longwall mining', *Coal Engineering*, Vol. 38, No. 1, pp.9–11.

Singh, G.S.P. and Singh, U.K. (2010) 'Prediction of caving behavior of strata and optimum rating of hydraulic powered support for longwall workings', *Int. J. Rock Mech. Min. Sci.*, Vol. 47, No. 1, pp.1–16.

Sun, Z., Zhang, Z., Wang, Z. et al. (2019) 'Application & research on hydraulic fracturing and cutting top pressure relief technology in large mining height retained roadway', *Coal Science and Technology*, Vol. 47, No. 10, pp.190–197.

Truemen, R., Lyman, G. and Cocker, A. (2008) 'Managing roof control problems on a longwall face', *Underground Coal Operators' Conference Wollongong*, 14–15 February, pp.9–21.

UDEC Universal Distinct Element Code (2011a) *Fish in UDEC*, Itasca Consulting Group, Inc.: Minneapolis, MI, USA.

UDEC Universal Distinct Element Code (2011b) *User's Guide*, Itasca Consulting Group, Inc., Minneapolis, MI, USA.

Van Dyke, M.A., Su, W.H. and Wickline, J. (2017) 'Evaluation of seismic potential in a longwall mine with massive sandstone roof under deep overburden', *Int. J. Min. Sci. Technol.*, Vol. 28, No. 1, pp.115–119.

Wang, B., Zhu, S., Jiang, F., Liu, J., Shang, X. and Zhang, X. (2020) 'Investigating the width of isolated coal pillars in deep hard-strata mines for prevention of mine seismicity and rockburst', *Energies*, Vol. 13, No. 17, p.4293.

Wang, H., Deng, D., Jiang, Y., Shi, R., Yang, G. and Zhang, X. (2021) 'Study on the dynamic evolution characteristics of deformation and collapse of the extra-thick hard roof', *Journal of Mining Science and Technology*, Vol. 006, No. 005, pp.548–557.

Wang, J., Yang, S., Yang, B. et al. (2019) 'Roof sub-regional fracturing and support resistance distribution in deep longwall face with ultra-large length', *Journal of China Coal Society*, Vol. 44, No. 1, pp.54–63.

Wei, B. (2020) 'Study on technology of hydraulic fracturing initial roof setting after fully-mechanized mining face support', *Coal Science and Technology*, Vol. 48, No. S1, pp.81–84.

Yu, J. (2022) 'Application of hydraulic fracturing technology in primary caving of mining face', *Shandong Coal Science and Technology*, Vol. 40, No. 6, pp.16–18.

Zhou, X., Ouyang, Z., Zhou, R., Ji, Z., Yi, H., Tang, Z., Chang, B., Yang, C. and Sun, B. (2021) 'An approach to dynamic disaster prevention in strong rock burst coal seam under multi-aquifers: a case study of Tingnan coal mine', *Energies*, Vol. 14, No. 21, p.7287.